

OFFICE OF NAVAL RESEARCH

GRANT: N00014-93-1-0757

R&T CODE 400X119YIP

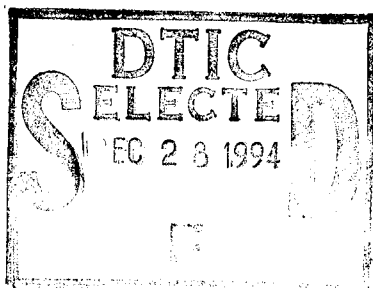
Dr. Robert J. Nowak

Technical Report No. 3

Self Assembly of n-Alkanethiolate Monolayers on Silver Nano-Structures:
Protective Encapsulation

by

Wenjie Li, Jorma A. Virtanen, and Reginald M. Penner



Prepared for Publication

in the Journal

Langmuir

University of California, Irvine
Department of Chemistry
Irvine, CA 92717-2025

December 18, 1994

Reproduction in whole or in part, is permitted for any purpose of the United States Government.

This document has been approved for public release and sale;
its distribution is unlimited.

19941223 012

DTIC QUALITY INSPECTED 1

REPORT DOCUMENTATION PAGE			Form Approved ONB No. 0704-0188	
Public reporting burden for this collection of information is estimated to average 1 hour per response, including the time for reviewing instructions, searching existing data sources, gathering and maintaining the data needed, and completing and reviewing the collection of information. Send comments regarding this burden estimate or any other aspect of this collection of information, including suggestions for reducing this burden, to Washington Headquarters Services, Directorate for Information Operations and Reports, 1215 Jefferson Davis Highway, Suite 1204, Arlington, VA 22202-4302, and to the Office of Management and Budget, Paperwork Reduction Project (0704-0188), Washington, DC 20503.				
1. AGENCY USE ONLY (LEAVE BLANK)		2. REPORT DATE Dec. 18, 1994		3. REPORT TYPE AND DATES COVERED Interim May 1993 - June 1994
4. TITLE AND SUBTITLE Self Assembly of n-Alkanethiolate Monolayers on Silver Nano-Structures: Protective Encapsulation			5. FUNDING NUMBERS N00014-93-1-0757	
6. AUTHOR(S) W. Li, J.A. Virtanen, and R.M. Penner				
7. PERFORMING ORGANIZATION NAME(S) AND ADDRESS(ES) University of California, Irvine Department of Chemistry Irvine, CA 92717-2025			8. PERFORMING ORGANIZATION REPORT NUMBER Technical Report No. 3	
9. SPONSORING/MONITORING AGENCY NAME(S) AND ADDRESS(ES) Office of Naval Research 800 North Quincy Street Arlington, VA 22217			10. SPONSORING/MONITORING AGENCY REPORT NUMBER R&T Number: 400X119YIP	
11. SUPPLEMENTARY NOTES				
12A. DISTRIBUTION AVAILABILITY STATEMENT Approved for public release, distribution unlimited			12B. DISTRIBUTION CODE	
13. ABSTRACT (Maximum 200 Words) Silver nanostructures having dimensions of 200-1000Å in diameter and 20-50Å in height were synthesized on graphite surfaces using the scanning tunneling microscope (STM). Although these nanostructures were stable while immersed in aqueous solutions containing small (0.5 mM) concentrations of Ag ⁺ , upon transfer into pure water, dissolution of the nanostructure occurred within 30 minutes, irrespective of the applied imaging bias up to ±200 mV. Anodic dissolution was inhibited following the formation of an n-alkane thiolate self-assembled monolayer (SAM) on the silver surface, demonstrating that molecular self-assembly provides a method for the protective, and chemically selective, encapsulation of reactive nanometer-scale structures on solid surfaces. Self-assembly was not observed following the exposure to long-chain n-alkyl amines or carboxylic acids.				
14. SUBJECT TERMS STM, n-alkane thiols, biological, lithography, passivation			15. NUMBER OF PAGES 22	
			16. PRICE CODE	
17. SECURITY CLASSIFICATION OF REPORT Unclassified	18. SECURITY CLASSIFICATION OF THIS PAGE Unclassified	19. SECURITY CLASSIFICATION OF ABSTRACT Unclassified	20. LIMITATION OF ABSTRACT Unlimited	

Self-Assembly of n-Alkanethiolate Monolayers on Silver Nanostructures: Protective Encapsulation

Wenjie Li, J.A. Virtanen, and R. M. Penner*

Institute for Surface and Interface Science (ISIS)

Department of Chemistry

University of California, Irvine

Irvine, CA 92717-2025

Abstract

Electrochemically synthesized silver nanostructures having dimensions of 200-1000Å in diameter and 20-50Å in height were prepared on graphite surfaces using the scanning tunneling microscope (STM). These nanostructures were stable while immersed in aqueous solutions containing small (0.5 mM) concentrations of Ag⁺ during repeated STM imaging at small sample-negative biases for at least one hour. Upon transfer into pure water, dissolution of the nanostructure occurred within 30 minutes, irrespective of the applied imaging bias up to ± 200 mV. The anodic dissolution of silver nanostructures in pure water was strongly inhibited following the formation of an n-alkane thiolate self-assembled monolayer (SAM) on the silver surface, demonstrating that molecular self-assembly provides a method for the protective, and chemically selective, encapsulation of reactive nanometer-scale structures on solid surfaces. In contrast, self-assembly was not observed following the exposure of silver nanostructures to long-chain n-alkyl amines or carboxylic acids and these prospective ligands provided no protection from dissolution of the nanostructure in pure water.

*Author to whom correspondence should be addressed.

<input checked="checked" type="checkbox"/>	
<input type="checkbox"/>	
<input type="checkbox"/>	
A-1	

Introduction

Recently, the scanning tunneling microscope (STM) has been employed to electrochemically deposit nanoscopic silver and copper disk-shaped structures having typical dimensions of 200-500Å in diameter and 20-100Å in height on graphite basal plane surfaces.¹⁻⁴ Metal deposition occurs via a two-step mechanism in which a shallow pit in the graphite surface is first formed⁵ followed immediately by electrochemical deposition of metal at this nucleation site.¹ The metal nanostructures prepared by this procedure are ideal candidates for investigations of stability and corrosion using *in-situ* STM imaging in part because these nanostructures are strongly anchored to the graphite surface and are immobile during repeated STM imaging.¹⁻⁴ In addition, each metal nanostructure protrudes from an atomically smooth graphite surface which is electrochemically unreactive. The graphite surface functions as a baseline against which small changes in the height of a metal nanostructure - resulting either from electrochemical reactions of the metal nanostructures,³ or from the adsorption of molecules from solution² - can be accurately measured. For example, we have previously demonstrated that the time dependence of the nanostructure height (measured with the STM in an aqueous solution) can be used to track the spontaneous electrochemical reactions of coexisting copper and silver nanostructures on graphite.³

Here we report the results of experiments in which the stability of silver nano-disk structures in dilute silver-ion-containing solutions and in pure water is compared. An important conclusion of this study is that in aqueous solution, silver nanostructures are inherently unstable in the absence of small concentrations (e.g. 0.5 mM) of silver ions. The observed instability of silver nanostructures provides a serious barrier to the preparation by electrochemical deposition of ensemble surface nanostructures composed of metals (or other materials) other than silver. Consequently, we have sought a method by which metal nanostructures might be stabilized in aqueous solutions in which ions of the metal are not present.

We have very recently reported² the results of experiments in which an n-alkanethiolate layer is self-assembled on the surface of silver nano-disk structures which were electrochemically deposited on graphite surfaces using our procedure. In this previous work, the thickness of the n-alkane thiolate monolayer was compared with the expected monolayer thickness based on two structural models for the monolayer.² Previously, n-alkanethiolate self-assembled monolayers (SAMs) have been employed as passivating layers for gold, silver, and copper surfaces exposed to air and solution.⁶⁻¹⁸ Here we report that n-alkanethiolate SAMs perform this same function at nanoscopic silver surfaces: Whereas silver nanostructures spontaneously dissolve in a deionized water ambient, following self-assembly of an n-alkane thiolate monolayer on a silver nanostructure, no erosion in the height (or volume¹⁹) of the structure was detected during exposures to deionized water of up to one hour. Other prospective ligands including two long-chain n-alkyl amines and a long-chain n-alkyl carboxylic acid were not observed to self-assemble at the silver surface. Exposure of silver nanostructures to these other ligands coincided with the onset of nanostructure height instability and rapid dissolution.

Experimental Section

STM imaging experiments were conducted using a modified Park Scientific Instruments AutoProbe cp STM/AFM in the conventional two electrode (i.e. tip and sample) mode. A Kel-F electrochemical sample holder permitted the exposure of a ≈ 6 mm diameter circular region of a graphite surface to a solution volume of ≈ 200 μ l. Flexible tygon tubing and a 20 ml syringe were employed to replace the AgF-containing plating solution with pure water during STM imaging investigations of silver nanostructure stability. STM tips were constructed from electrochemically etched 0.5 mm diameter platinum wire which was coated with poly- α -methyl styrene polymer as previously described.²⁰ The output from an arbitrary waveform generator (Stanford

Model DS340) was added to the sample potential in order to effect silver nanostructure deposition as described below.

Silver nano-disks were grown electrochemically on graphite surfaces using previously described procedures.^{1,3,4} Briefly, electrochemical growth of silver nanostructures was induced by the application of 6.0 V x 50 μ sec (tip-positive) bias voltage pulses from the arbitrary waveform generator between the STM tip and a graphite surface immersed in aqueous 0.5mM AgF (Aldrich, >99.99%). The bias pulse induced the electrochemical growth of a nanoscopic silver adsorption site by a two step mechanism involving the formation of a monolayer-deep pit in the graphite surface within \approx 5 μ sec of the application of the bias pulse, and the subsequent diffusion-controlled deposition of silver until the termination of the pulse at 50 μ sec.¹

Following the deposition and *in-situ* characterization of the deposit by STM imaging, the ligand of interest was introduced into the STM using either of two methods: For liquids ($n \leq 16$), 20 μ l of neat ligand was injected into \approx 200 μ l of the aqueous 0.5 mM silver plating solution contained in the Kel-F sample holder in the STM. Following injection, approximately five minutes elapsed before high magnification STM images of the nanostructure could be reacquired. Alternatively, n-octadecane thiol - a solid at room temperature - was introduced as a solution in n-octane using the same technique. Following introduction into the STM electrochemical cell, this n-octane solution floated as a thin film on the surface of the aqueous electrolyte in the cell, and partitioning of the n-alkane thiol into the electrolyte occurred.

Results and Discussion.

In-situ STM imaging is one method by which the stability of immobilized metal particles may be investigated. The silver nanostructures prepared using the method outlined above are particularly attractive candidates for these investigations since - as previously demonstrated¹⁻⁴ - these particles are anchored to the graphite substrate

surface at defect sites and are immobile during repeated STM imaging in aqueous solutions. In a previous paper, we demonstrated that either silver or copper nanostructures are stable when imaged in dilute solutions of their respective ions at tip-sample biases which are small (20-40 mV) and tip-positive.⁴ For the silver nanostructures which are the subject of this paper, this fact is confirmed in the experiment of Figure 1. Figure 1A shows STM images of a silver nanostructure synthesized using a single -6.0 V x 50 μ sec bias pulse. This nanostructure possessed an unusually distinctive and complicated shape which increases the likelihood that either small additions or subtractions of silver resulting from electrochemical reactions will be observable in STM images. The same particle is shown 32 minutes later in Figure 1B following the acquisition of 20 STM images using an imaging bias of +24 mV (tip vs. sample) and a set-point current of 0.8 nA. No changes in the height or the apparent volume of the nanostructure were observed within the reproducibility of this measurement of approximately $\pm 5 \text{ \AA}$ in height and $\pm 200 \text{ \AA}^3$ in volume.

This stability observed during STM imaging at sample-negative biases is not retained for tip-negative biases of 20-40 mV.¹ In this case, dissolution of silver nanostructures is usually observed. In other words, a change of the imaging bias of 40 mV (from +20 mV to -20 mV) induces a transition to instability from stability for silver nanostructures immersed in 0.5 mM AgF. This observation suggests that the open-circuit potential of the graphite surface in these experiments is within 40 mV of the Nernst potential for silver when the surface is in contact with a dilute aqueous Ag⁺-containing solution although only a few nanostructures are present on the graphite surface.¹ In fact, the potential of the graphite surface with attached silver nanostructures can be directly measured versus a silver wire using a high impedance voltmeter and this potential is typically within 5 mV of a silver wire reference immersed in the same aqueous, 0.5 mM AgF solution. The effect of an applied imaging bias of ± 20 mV is therefore to displace the graphite surface in potential either in the direction of anodic

dissolution or in the direction of silver metal deposition, however the rate of the resulting cathodic polarization is clearly not appreciable (because in experiments like that shown in Figure 1, no increase in the nanostructure dimension is detected). The tip-sample imaging bias therefore provides control over the nanostructure stability even in the simplest two-electrode *in-situ* STM imaging configuration.

It is important to recognize that the Nernst potential for silver nanostructures will only be defined in the presence of silver ion in the contacting aqueous solution. When the silver ion-containing solution is replaced with pure water, silver dissolution commences and the dimensions of silver nanostructures become smaller with time. In Figure 2A, for example, a silver nanostructure having a height of $\approx 65\text{\AA}$ is shown immediately following electrochemical deposition in aqueous 0.5 mM AgF . Following transfer from the 0.5 mM AgF plating solution to pure water, the STM images shown in Figures 2B and 2C, taken at intervals of 6 minutes and 30 minutes after transfer, show an obvious decrease in height. A plot of the average height versus time shown in Figure 2D reveals a decrease from 64 \AA to 26 \AA over the course of thirty minutes following transfer to pure water. The dissolution of metal nano-dots is reproducibly observed upon exposure to pure water for nanostructures of cadmium and copper as well as silver at imaging biases of $\approx 30\text{ mV}$. This instability is due to the positive drift of the electrochemical potential of the surface from the reversible Nernst potential for the metal and its ions, because the Nernst potential of the surface is undefined in pure water. This potential drift of the surface relative to a reference electrodes is experimentally measurable, and it is not eliminated by increasing the STM imaging bias voltage to values as high as $+200\text{ mV}$.

Previously we have shown that if instead of pure water, aqueous 0.5 mM Cu^{2+} is substituted for the silver plating solution and copper nanostructures are deposited, a spontaneous electrochemical reaction occurs in which a few monolayers of copper plate onto the silver nanostructures.³ Designed nanometer-scale electrochemical reactions

such as this galvanic discharge have many potential applications, however electrochemical “cross-talk” of this type can also be undesirable during electrochemical nano-fabrication since contamination of nanostructures can occur.

A well-known strategy for protecting metal surfaces from corrosion is to apply a coating which blocks electronic and ionic conduction to a contacting aqueous phase and restricts access of uncharged reactants such as water and O_2 to the metal surface. Previously it has been demonstrated that for macroscopic surfaces of copper¹³ and gold,^{6,9,14,15,17,21,22} a single self-assembled monolayer (SAM) of n-alkane thiol molecules effectively accomplishes one or more of these functions provided the alkyl chain length of the thiols is approximately C_8 or greater. In the context of electrochemical nanofabrication experiments on graphite surfaces, n-alkanethiolate monolayers are expected to spontaneously and selectively assemble at nanostructures composed of silver, copper, gold, and silver, but not on the graphite surface which is inert to thiol chemisorption. For silver nanostructures, this expectation is confirmed by the data of Figure 3: An STM image of two silver nanostructures immersed in the aqueous 0.5 mM AgF solution from which they were deposited is shown in Fig. 3A. The cross sections shown in Fig. 3D reveals the diameters of these structures are approximately 500Å and 300Å, respectively. The nanostructure dimensions apparent in Figure 3D were stable to within $\pm 5\%$ for a period of approximately 30 minutes during repetitive STM imaging in this solution at an applied bias of +24mV. In Figure 3B, the same nanostructures are shown following exposure to an aqueous solution saturated with dodecane thiol ($CH_3(CH_2)_{11}SH$), transfer to a pure water ambient, and exposure for ten minutes during the acquisition of nine STM images. The cross-section shown in Fig. 3D (marked “after”) shows that in contrast to the deterioration in height normally observed following exposure to pure water, the maximum heights of both nanostructures have increased to near 40Å.

Recently, we have reported that for a series of n-alkyl thiols varying in length from C₁₀ (all-trans length $\approx 16\text{\AA}$) to C₁₈ ($\approx 26\text{\AA}$), the step-wise height increase observed for silver nanostructures following thiol exposure increases linearly with the n-alkyl chain length.² For the longest members of this series (C₁₆ and C₁₈) which are well below their respective chain melting transition temperatures at room temperature, the observed height increment approximately equals the expected all-trans chain length for these thiols indicating that little STM tip penetration into the thiolate layer occurs during imaging. This result was obtained using tunneling currents of 0.2-0.8 nA and tip-positive imaging biases of ≈ 40 mV corresponding to a tunneling gap resistance in the interval from 50-200 M Ω . The height increases observed for the two nanostructures shown in Figure 3 are approximately 15\AA following exposure to dodecane thiol (all-trans length $\approx 18.7\text{\AA}$) which is consistent with our previously reported results.²

Following thiol exposure and SAM formation, the thiol-containing electrolyte was replaced with deionized water. A plot of the nanostructure height versus time shown in Figure 3D shows that no detectable dissolution of the nanostructure occurs for the ensuing 30 minute exposure to water (and for an additional 30 minutes which are not plotted in Figure 3D). The apparent stability in water of the nanostructures shown in Figure 3 is attributed to the insulation of the silver surface from ions and solvent by the n-alkane thiolate SAM. The stabilization of silver nanostructures in pure water was observed following the exposure of silver nanostructures to any of five different n-alkane thiols having alkyl chain lengths of C₁₀, C₁₂, C₁₄, C₁₆, and C₁₈. These experiments demonstrate silver nanostructures may be protected from dissolution by encapsulation in a protective n-alkanethiolate SAM.

Although it is likely that the SAM imposes a physical barrier to ion transport with dissolved species in solution, the n-alkanethiolate monolayer may also modify the reactivity of silver nanostructures via an electronic mechanism. Chemisorption of a nucleophilic thiol molecule on silver is accompanied by charge donation to the metal.

The cumulative effect of the adsorption of many thiol molecules is a negative shift of the Fermi level which is predicted to be appreciable (e.g., $\approx 0.40\text{eV}^{23}$) for silver colloids having diameters of a few angstroms. Henglein and coworkers^{23,24} have recently invoked this mechanism to account for the increased reactivity of silver colloids toward dissolved O_2 , and changes in the absorption spectrum for these colloids, following exposure to SH^- . For the much larger silver nanostructures which are the topic of the present work, the magnitude of the negative shift of the Fermi energy brought about by electron donation from adsorbed thiols is readily estimated. In the context of a free-electron gas approximation, the Fermi energy, ε_F , of a metal nanostructure is related to the nanostructure volume, V , and the total number of electrons, N , by:²⁵

$$\varepsilon_F = \frac{\hbar^2}{2m} \left(3\pi^2 \frac{N}{V} \right)^{2/3} \quad (1)$$

where m is the electron mass. An increase of N by a small fraction, x , results in a change of the Fermi energy given by:²⁶

$$\Delta\varepsilon_F = \frac{2}{3} \varepsilon_F x \quad (2)$$

The fraction, x , can be estimated as the product of three terms: the fraction of the total number of atoms in a nanostructure (N) which are surface atoms, (n_s); the fraction of surface atoms on which are bonded an alkane thiolate adsorbate; and the fractional charge associated with each chemisorption bond, δe . Assuming that the $\sqrt{3}x\sqrt{3}\text{R}30^\circ$ ordering of alkane thiolate molecules on $\text{Au}(111)^{27,28}$ approximately obtains for the silver nanostructures investigated here, 1/3 of all surface atoms are directly bonded to a thiol molecule. x is therefore given by:

$$x = \frac{1}{3} \frac{n_s}{N} \delta \quad (3)$$

and $\Delta\epsilon_F$ is:

$$\Delta\epsilon_F = \frac{2}{9} \epsilon_F \frac{n_s}{N} \delta \quad (4)$$

For a disk-shaped silver nanostructure having typical dimensions of 500 Å in diameter and 50 Å in height (as shown, for example in Figure 2), the surface area and volume are $1.6 \times 10^5 \text{ Å}^2$ (or $1.6 \times 10^{-11} \text{ cm}^2$) and $9.8 \times 10^6 \text{ Å}^3$ (or $9.8 \times 10^{-18} \text{ cm}^3$) corresponding to $n_s = 1.8 \times 10^4$ silver atoms and $N = 5.8 \times 10^5$ silver atoms, respectively. If ϵ_F and δ are taken to be 5.48 eV and 0.3, respectively²⁶, Eq. 4 yields a negative shift of 11 meV. Electronic stabilization of this order is unlikely to affect the outcome of the silver nanostructure dissolution experiment.

In addition to thiols, other ligands which complex silver ions may be strongly adsorbed at silver nanostructures and these ligands also have the potential to modify reactivity. Two other candidates are n-alkyl amines and carboxylic acids. Figure 4 shows the effect on the silver nanostructure height of the addition of C₁₀ and C₁₈ n-alkyl carboxylic acids and a C₁₈ amine to the pH=6.0 aqueous 0.5 mM AgF solution employed for deposition. Also shown for purposes of comparison are representative experiments involving water exposure in the absence of a ligand and n-alkane thiolate exposure for n-octadecane thiolate. Only following exposure to n-octadecane is an increase in the nanostructure height observed as a consequence of monolayer self-assembly. Exposure to either of the carboxylic acids or the amine coincided with an immediate onset of height instability and the eventual dissolution of the nanostructure in 20-40 minutes. As shown in the plots of Figure 4, this instability mimics the behavior observed for unprotected silver nanostructures exposed to pure water. Based on this similarity, it is likely that this ligand induced instability derives from the lowering of the

free silver ion concentration in solution caused by the formation of soluble silver complexes.

Summary

The protective encapsulation of silver nanostructures by self-assembled monolayers of n-alkane thiols has been demonstrated. For unmodified silver nanostructures having typical dimensions of 200-1000Å in diameter and 20-50Å in height, nanostructure dimensions are unaffected by STM imaging at modest, sample-negative biases of 20-40 mV in dilute silver ion-containing solutions having $[Ag^+] \approx 0.5$ mM. Replacement of the silver electrolyte with pure water, however, causes an immediate onset of instability and the rapid dissolution of the nanostructure within thirty minutes - irrespective of the applied imaging bias up to +200 mV.

The exposure of graphite-supported silver nanostructures to aqueous solutions of n-alkane thiolates results in the spontaneous self-assembly of monolayers on these structures. Following thiol exposure, SAM formation is immediately apparent as a step-wise increase in the nanostructure height as previously described.² Following SAM formation, the dissolution of silver nanostructures following exposure to pure is strongly inhibited for durations of exposure of up to one hour. The nanostructure capping strategy demonstrated here is expected to afford new flexibility in the preparation of ensembles of nanostructures composed of different materials using a variety of synthetic methods.

Acknowledgment. The authors gratefully acknowledge the financial support of this work by the Office of Naval Research (#400XYIP119) and the National Science Foundation (#DMR-9257000). The highly oriented pyrolytic graphite employed in this work was generously donated by Art Moore of Advanced Ceramics, Inc. In addition, J.A.V. thanks the Finnish Cultural Foundation for financial assistance.

Figure Captions

Figure 1 - STM images of a silver nanostructure electrochemically deposited on a graphite surface: **A.** The silver nanostructure is shown immediately following deposition in an aqueous solution of 0.5 mM AgF. **B.** The same silver nanostructure is shown following 32 minutes and the acquisition of 20 STM images. Both images were acquired using an imaging bias, $E_B = 24$ mV (tip positive) and a tunneling current, $i_t = 0.8$ nA.

Figure 2 - STM images of a silver nanostructure electrochemically deposited on a graphite surface: **A.** The silver nanostructure is shown immediately following deposition in an aqueous solution of 0.5 mM AgF. Deposition was effected by the application of a single, tip-positive bias pulse of 6V x 50 μ sec between the STM tip and the graphite surface in this solution. **B.** The same nanostructure immediately (i.e., within 1 minute) following transfer to a pure water solution, and, **C.** after ≈ 5 minutes in pure water. All images were acquired using an imaging bias, $E_B = 30$ mV (tip positive) and a tunneling current, $i_t = 0.6$ nA. **D.** Plot of the average height of the silver nanostructure shown in Figure 2 versus time showing the monotonic deterioration of the nanostructure height.

Figure 3 - STM images of two silver nanostructures electrochemically deposited on a graphite surface: **A.** The silver nanostructures are shown immediately following deposition in an aqueous solution of 0.5 mM AgF. **B.** The same nanostructures are shown following the addition of n-decane thiol to this solution, transfer to pure water, and exposure to the pure water ambient for ≈ 20 minutes. All images were acquired using an imaging bias, $E_B = 30$ mV (tip positive) and a tunneling current, $i_t = 0.6$ nA.

Figure Captions (con't)

Figure 3 (con't): C. Cross-sections for the nanostructures shown in A (labeled before...) and B (labeled after) are shown. D. Plot of the average heights of both nanostructures as a function of time during the exposure of these nanostructures to dodecane thiol, and the transfer to a pure water ambient.

Figure 4 - Plots of the average height of five different nanostructures following exposure to various ligands and deionized water: ● \equiv $\text{CH}_3(\text{CH}_2)_{16}\text{COOH}$; □ \equiv $\text{CH}_3(\text{CH}_2)_{17}\text{SH}$ where; (open diamond) \equiv $\text{CH}_3(\text{CH}_2)_8\text{COOH}$; (grey, open diamond) \equiv $\text{CH}_3(\text{CH}_2)_{17}\text{NH}_2$; and, ○ \equiv deionized water.

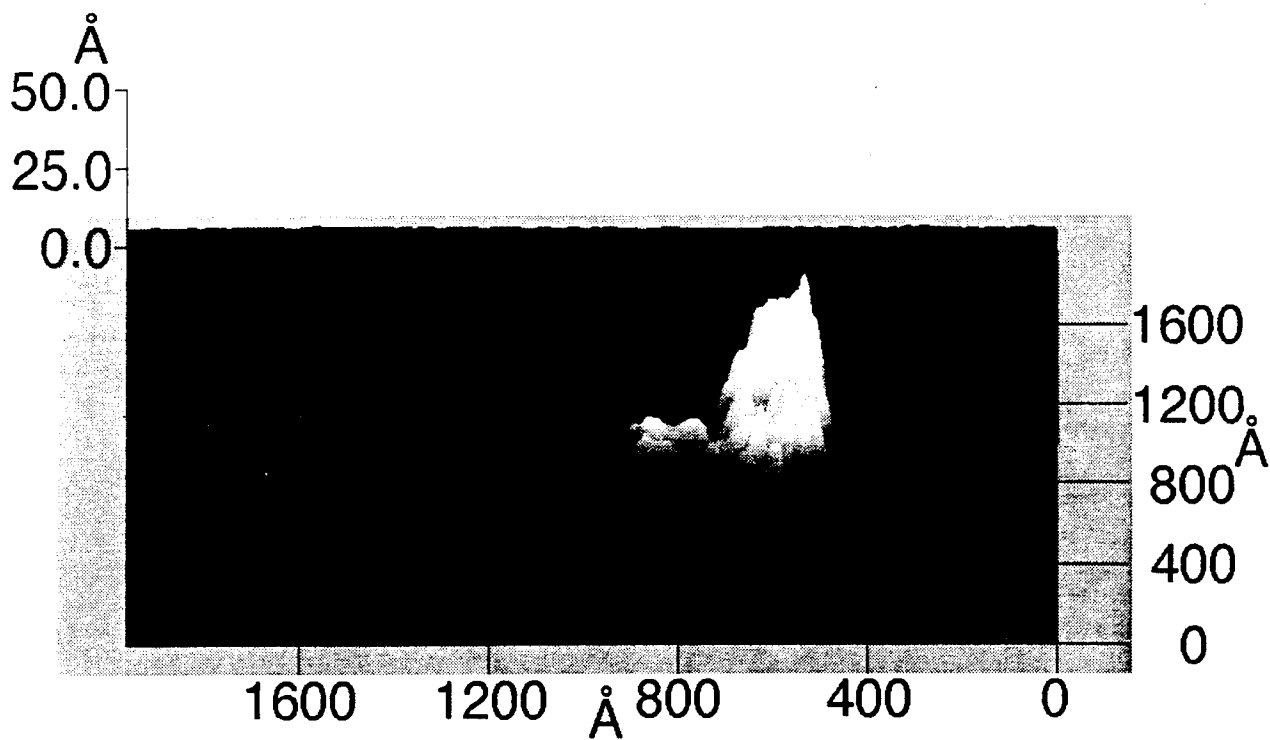
References and Notes

- (1) Li, W.; Duong, T.; Virtanen, J. A.; Penner, R. M. *Proc. NATO ASI 1993* in press.
- (2) Li, W.; Virtanen, J. A.; Penner, R. M. *J. Phys. Chem.* **1994**, *98*, 11751.
- (3) Li, W.; Virtanen, J. A.; Penner, R. M. *Appl. Phys. Lett.* **1992**, *60*, 1181.
- (4) Li, W.; Virtanen, J. A.; Penner, R. M. *J. Phys. Chem.* **1992**, *96*, 6529.
- (5) Penner, R. M.; Heben, M. J.; Lewis, N. S.; Quate, C. F. *Appl. Phys. Lett.* **1991**, *58*, 1389.
- (6) Chidsey, C. E. D.; Loiacono, D. N. *Langmuir* **1990**, *6*, 682.
- (7) Chidsey, C. E. D. *Science* **1991**, *251*, 919.
- (8) Finklea, H. O.; Robinson, L. R.; Blackburn, A.; Richter, B.; Allara, D.; Bright, T. *Langmuir* **1986**, *2*, 239.
- (9) Finklea, H. O.; Avery, S.; Lynch, M.; Furtch, T. *Langmuir* **1987**, *3*, 409.
- (10) Kumar, A.; Biebuych, H. A.; Abbott, N. L.; Whitesides, G. M. *J. Am. Chem. Soc.* **1992**, *114*, 9188.
- (11) Kumar, A.; Whitesides, G. M. *Appl. Phys. Lett.* **1993**, *63*, 2002.
- (12) Kumar, A.; Whitesides, G. M. *Science* **1994**, *263*, 60.
- (13) Laibinis, P. E.; Whitesides, G. M. *J. Am. Chem. Soc.* **1992**, *114*, 9022.
- (14) Porter, M. D.; Bright, T. B.; Allara, D. L.; Chidsey, C. E. D. *J. Am. Chem. Soc.* **1987**, *109*, 3559.
- (15) Rubinstein, I.; Steinberg, S.; Tor, Y.; Shanzer, A.; Sagiv, J. *Nature* **1988**, *332*, 426.
- (16) Sabatini, E.; Rubinstein, I.; Maoz, R.; Sagiv, J. *J. Electroanal. Chem.* **1987**, *219*, 365.
- (17) Sabatini, E.; Rubinstein, I. *J. Phys. Chem.* **1987**, *91*, 6663.
- (18) Sun, L.; Crooks, R. M. *Langmuir* **1993**, *9*, 1951.
- (19) It is widely appreciated that the volume of a protrusion on a surface, estimated by integrating STM line scans, actually provides an upper limit to the volume. The

apparent nanostructure volume obtained by this method equals the true nanostructure volume only in the limits of a small tip radius, a high tip aspect ratio, and a high density of STM line scans (in the slow scan direction of STM image acquisition). The effect of finite STM tip size is to exaggerate the dimensions of protrusions on a surface. Conclusions based on absolute nanostructure volumes are therefore potentially misleading and in this work, conclusions are derived only from changes in the nanostructure volume and geometry which are observed with time. These conclusions are subject to the assumption that the geometry of the platinum STM tip is invariant over the duration of the experiment.

- (20) Penner, R. M.; Heben, M. J.; Lewis, N. S. *Anal. Chem.* **1989**, *61*, 1630.
- (21) Steinberg, S.; Rubinstein, I. *Langmuir* **1992**, *8*, 1183.
- (22) Chailapakul, O.; Sun, L.; Xu, C.; Crooks, R. M. *J. Am. Chem. Soc.* **1993**, *115*, 12459.
- (23) Mulvaney, P.; Linnert, T.; Henglein, A. *J. Phys. Chem.* **1991**, *95*, 7843.
- (24) Henglein, A.; Linnert, T.; Mulvaney, P. *Ber. Bunsenges. Phys. Chem.* **1990**, *94*, 1449.
- (25) Kittel, C. *Introduction to Solid State Physics*; 6th ed.; John Wiley & Sons: New York, 1986.
- (26) Henglein, A. *J. Phys. Chem.* **1993**, *97*,
- (27) Chidsey, C. E. D.; Liu, G. Y.; Rowntree, P.; Scoles, G. *J. Chem. Phys.* **1989**, *91*, 4421.
- (28) Strong, L.; Whitesides, G. M. *Langmuir* **1988**, *4*, 546.

A.



B.

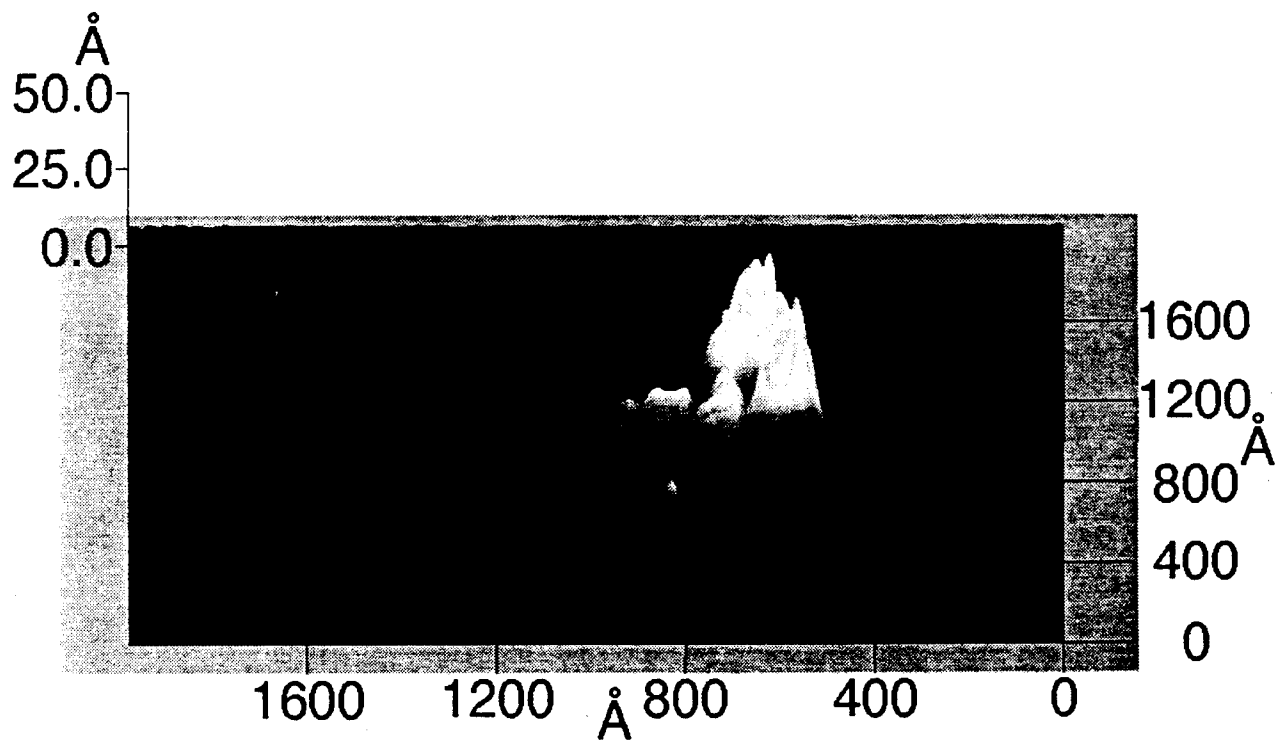


Figure 1. Li et al., ISIS, Dept. of Chem., UCI

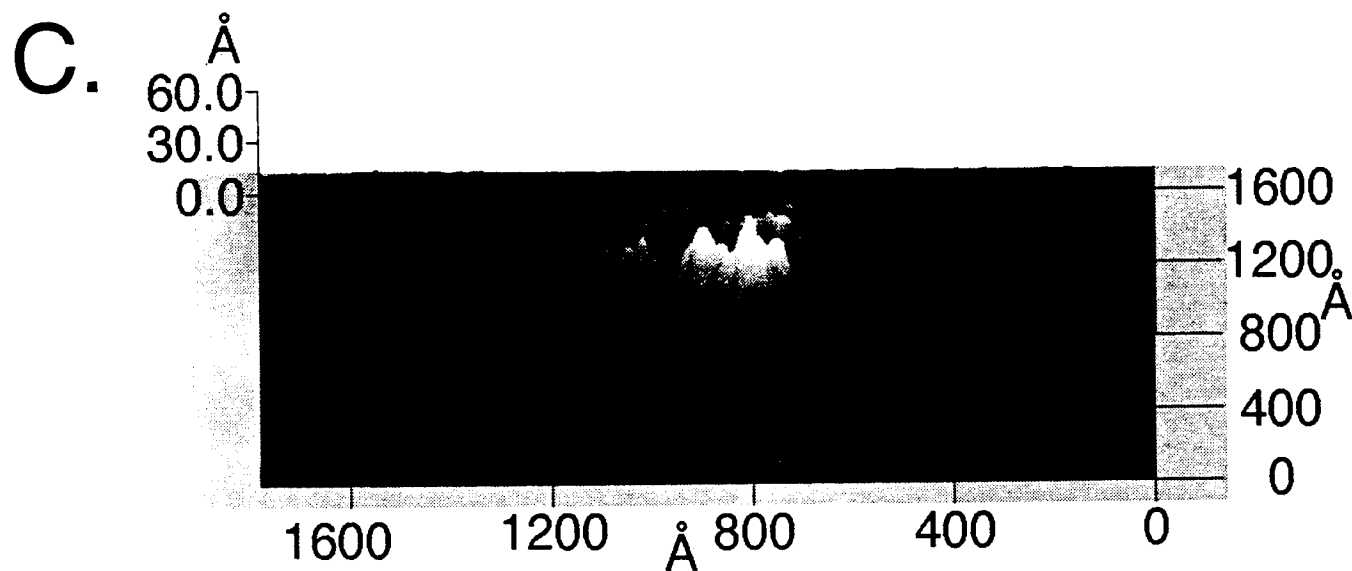
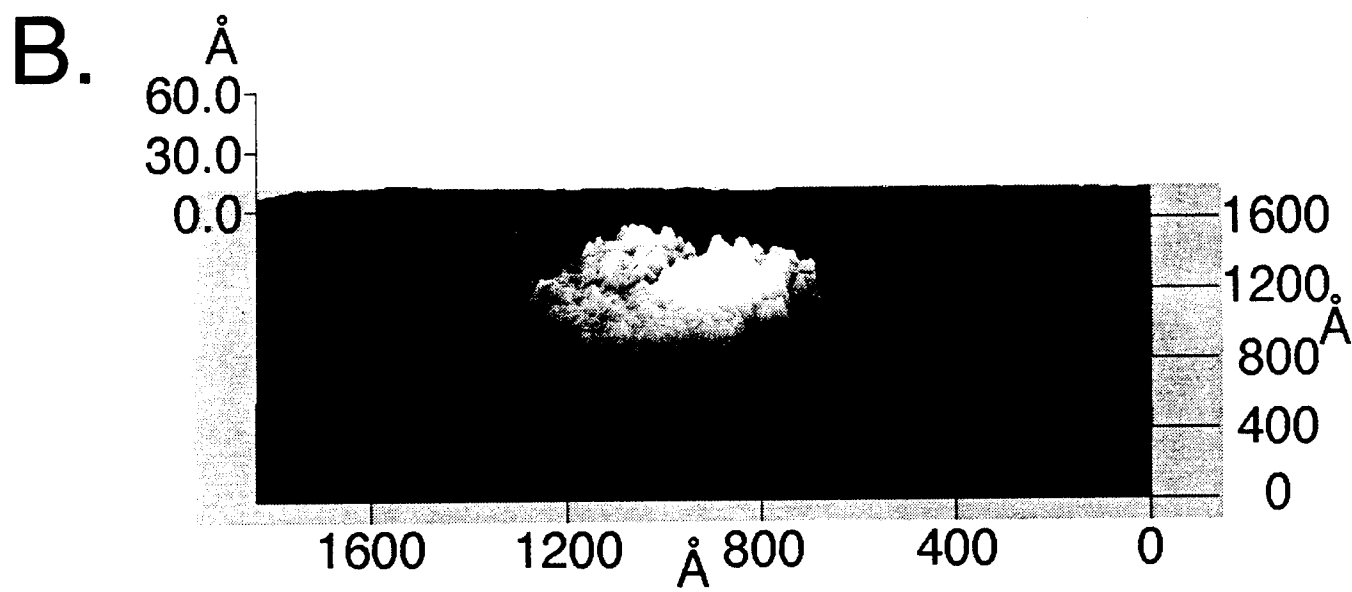
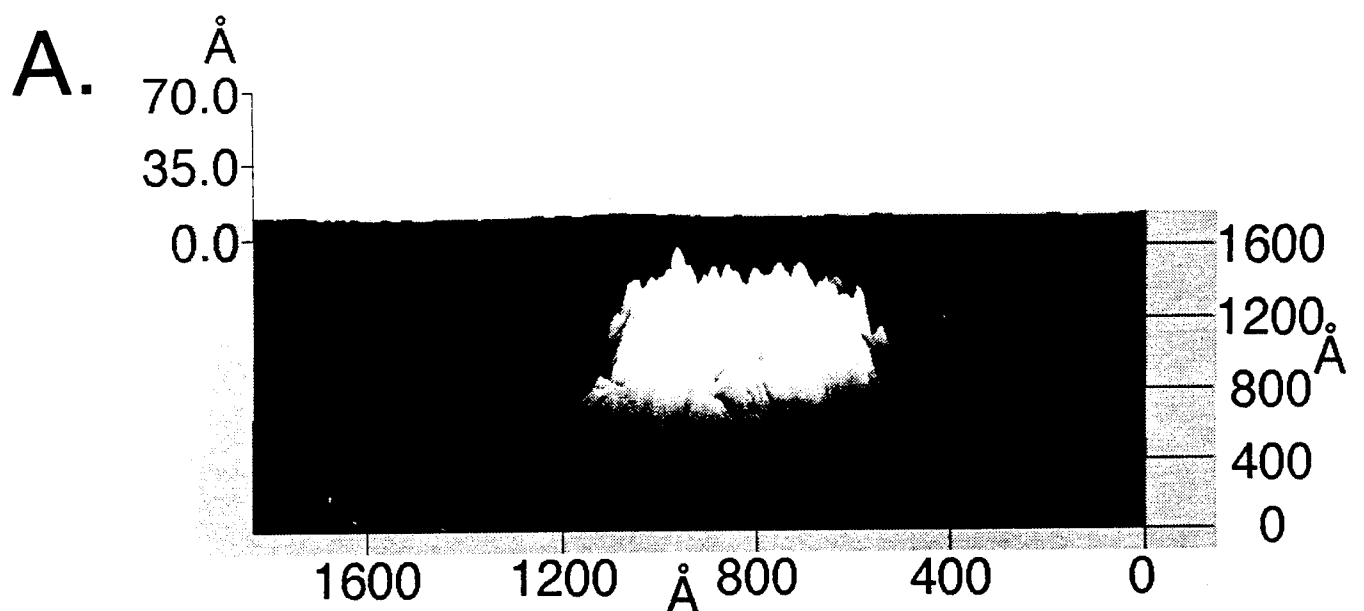


Figure 2A-C. Li *et al.*, ISIS, Dept. of Chem., UCL

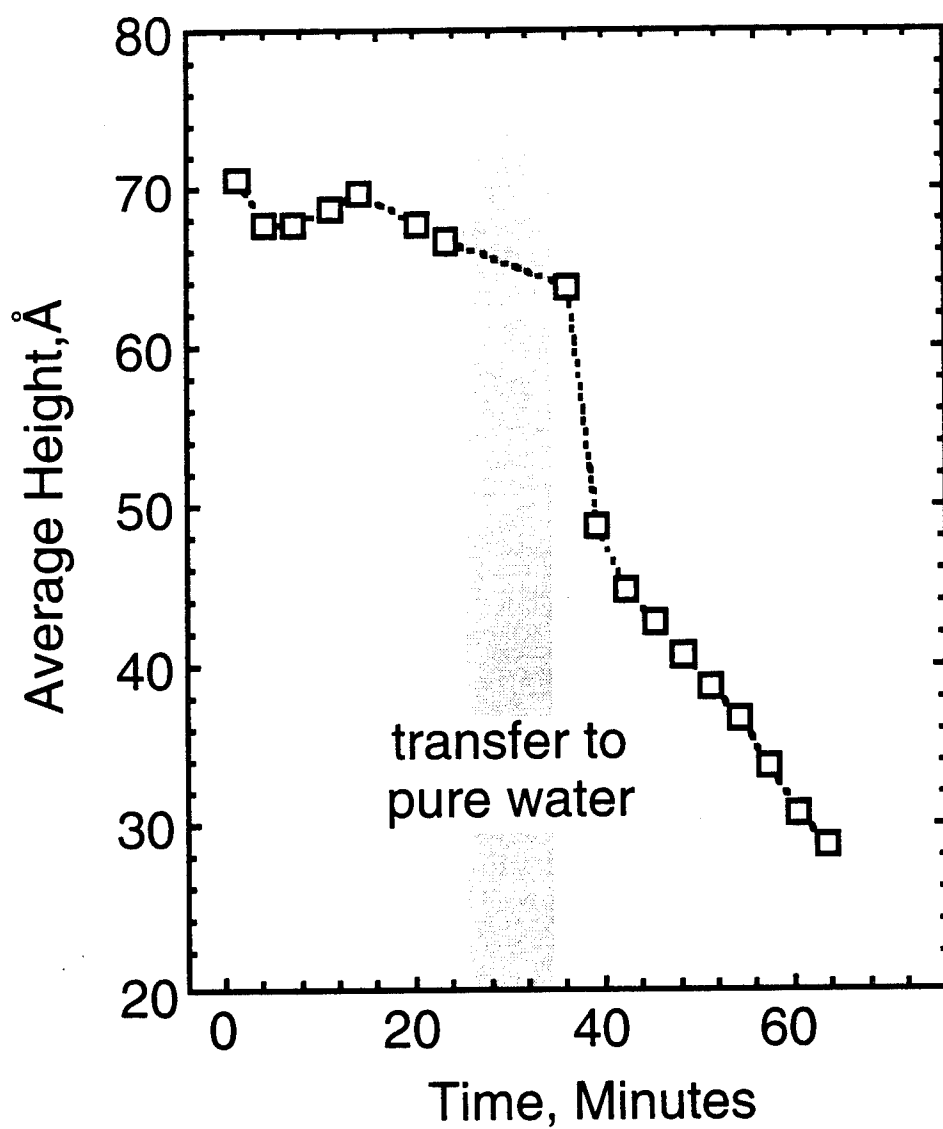
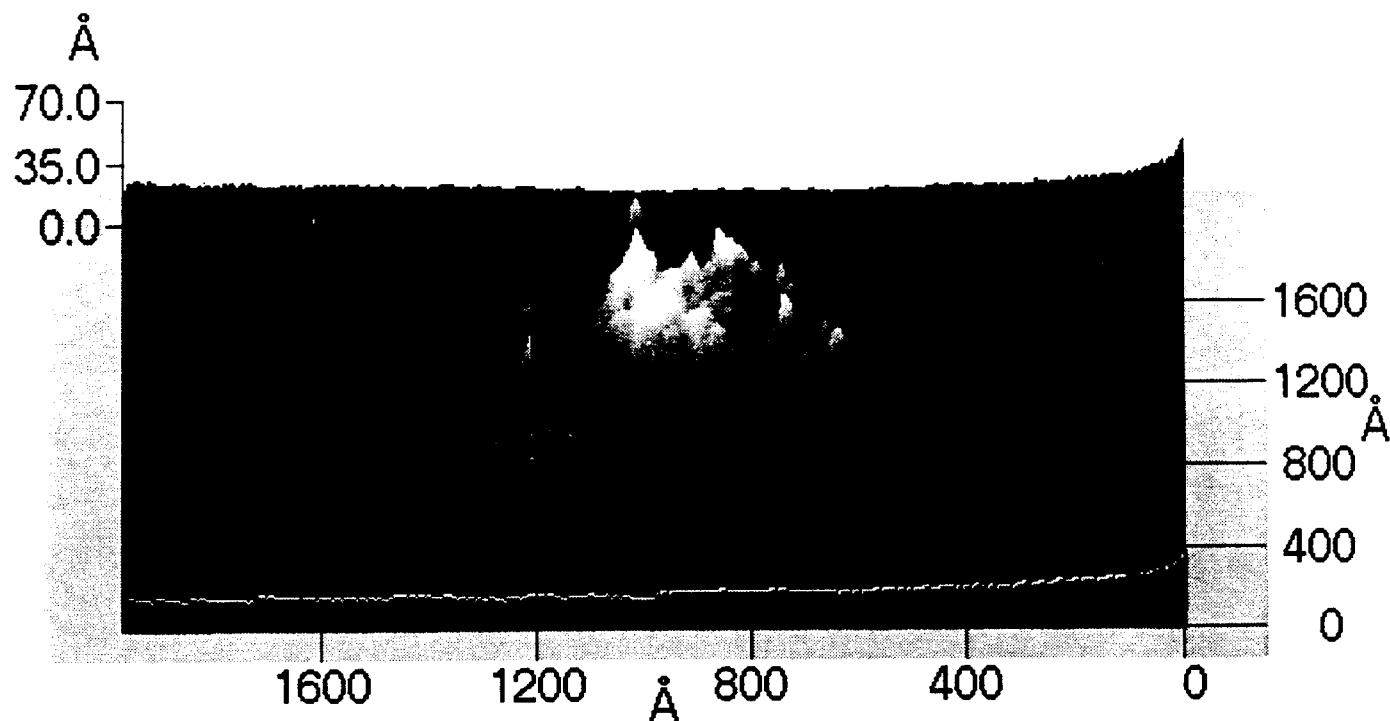


Figure 2D. Li et. al., ISIS, Dept. of Chem. UCI

A.



B.

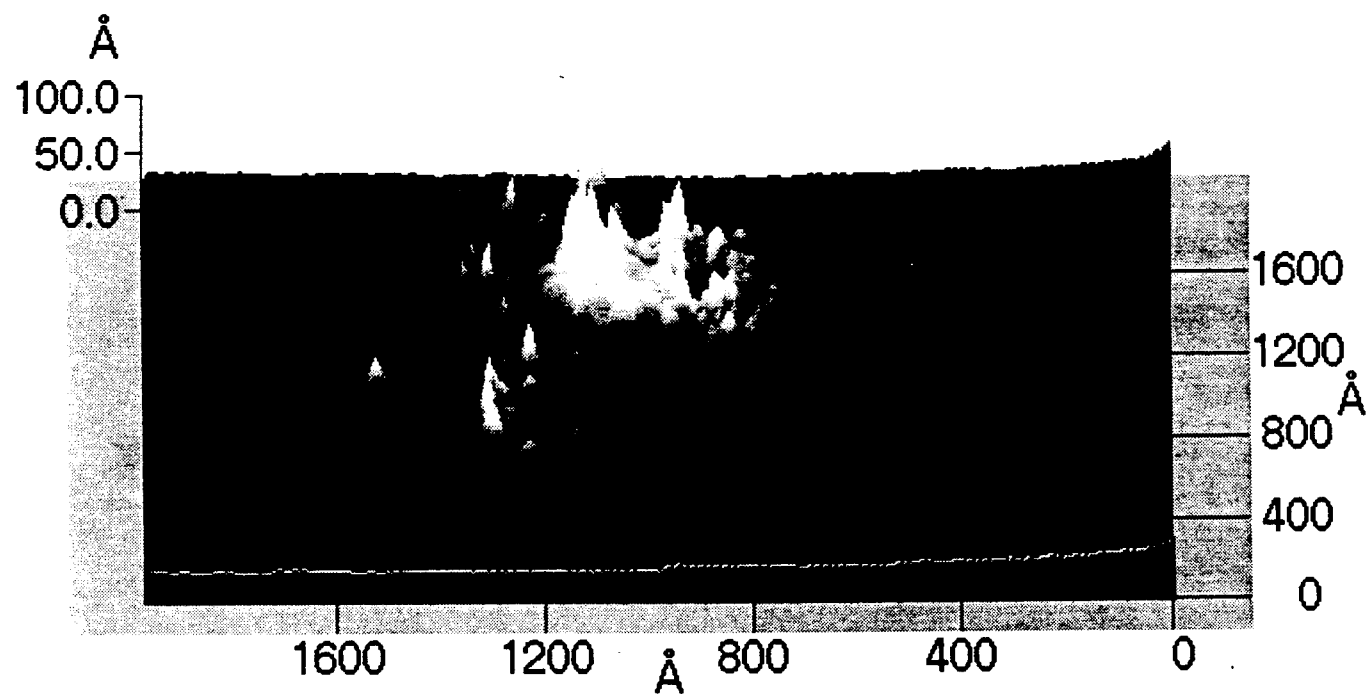


Figure 3. Li et al., ISIS, Dept. of Chem., UCI

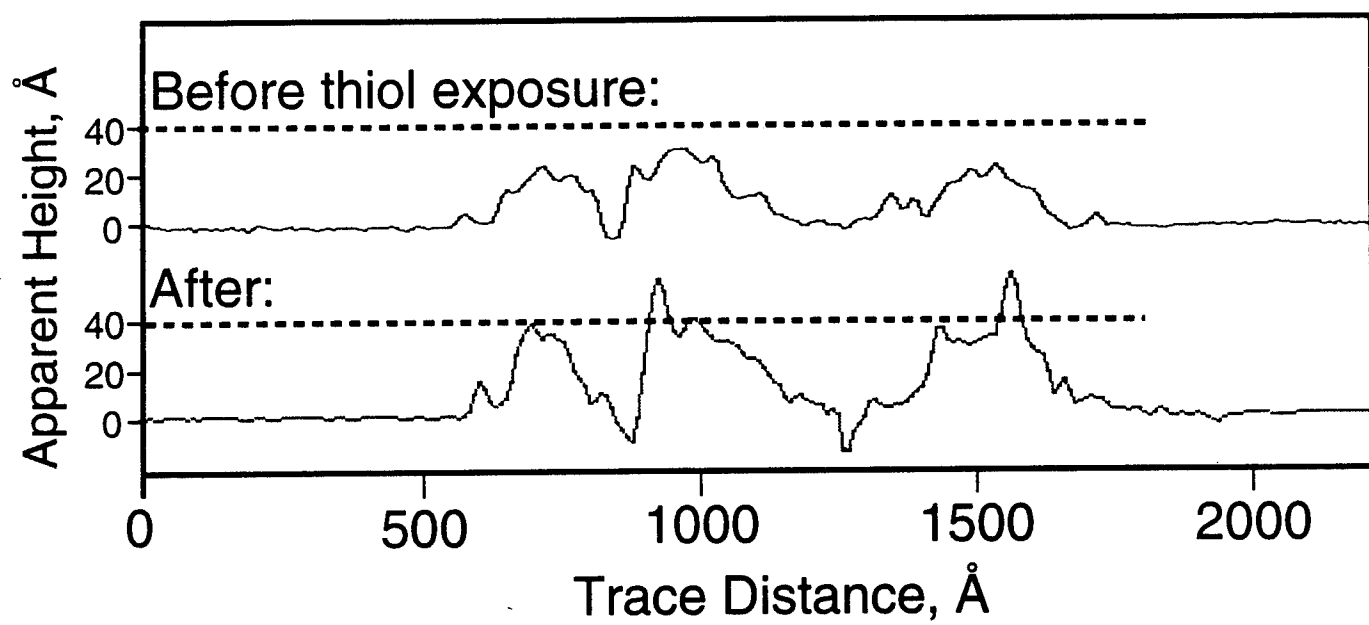


Figure 3C. Li *et al.*, *ISIS*, Dept. of Chem., UCI

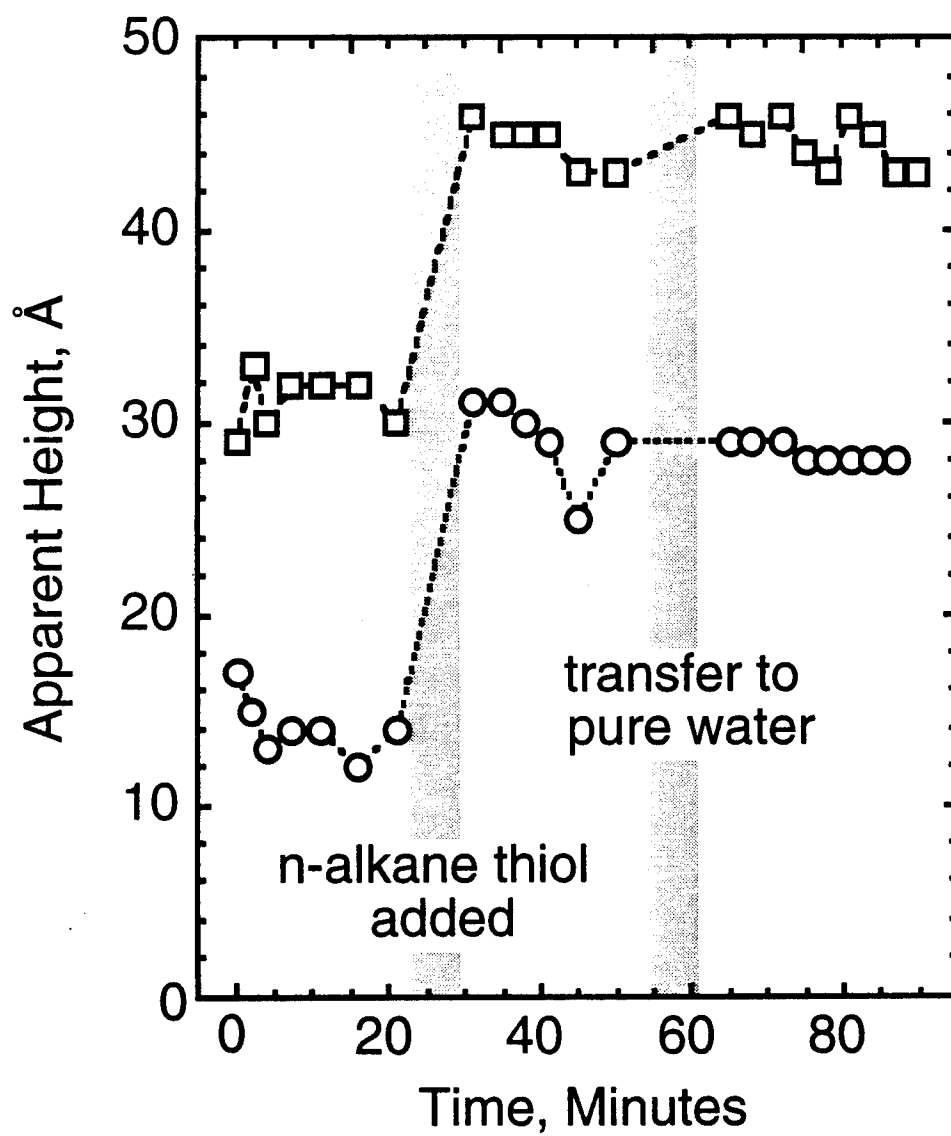


Figure 3D - Li et al., ISIS, Dept. of Chem., UCL

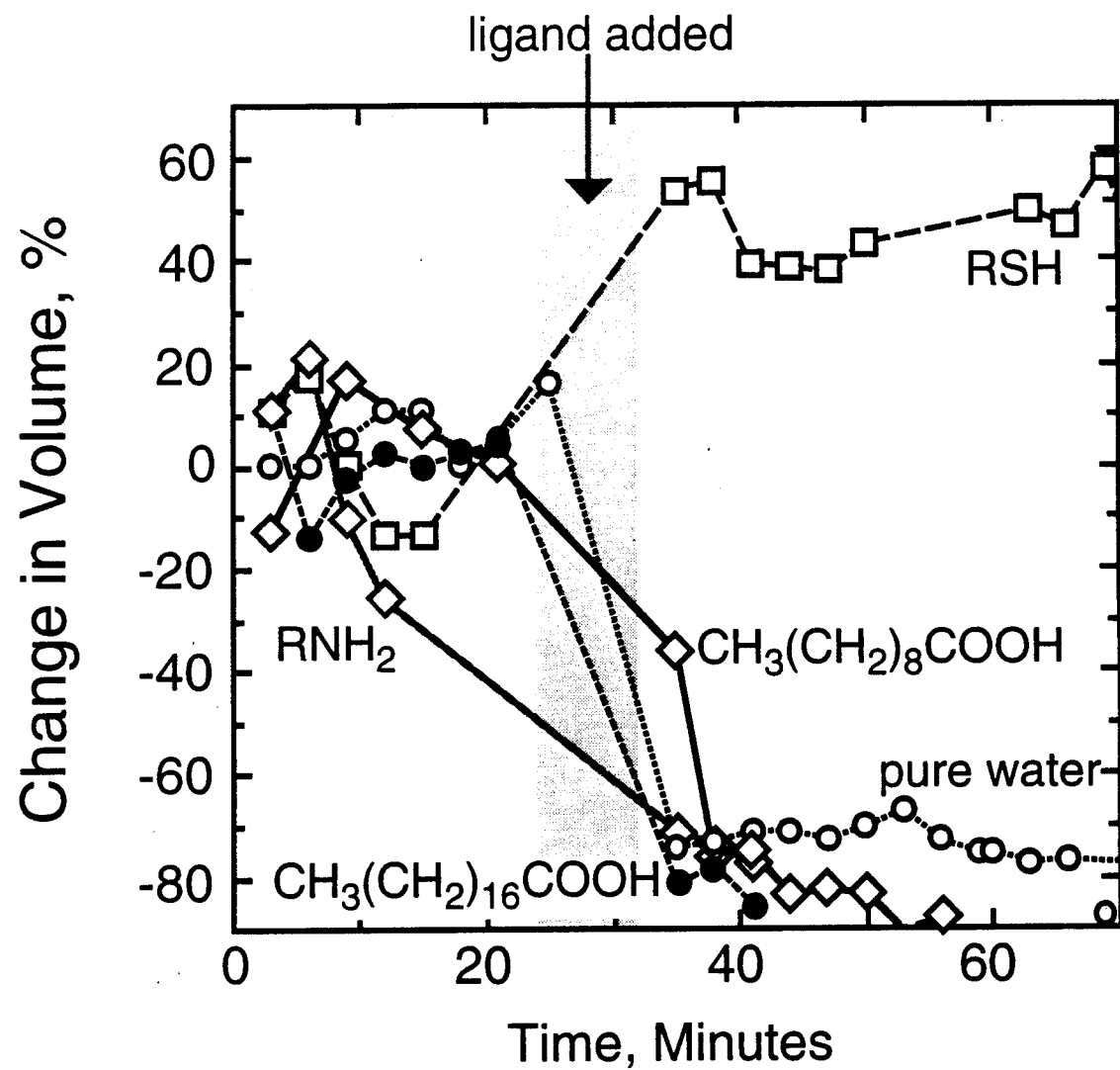


Figure 4. Li et al., ISIS, Dept. of Chem., UCI